Jesús Esteban*, Félix García-Ochoa and Miguel Ladero

Solventless synthesis of solketal with commercially available sulfonic acid based ion exchange resins and their catalytic performance

Abstract: As a means to valorize glycerol, the synthesis of solketal through a ketalization reaction with acetone was performed. Mild solventless conditions were applied to test the activity of different commercially available sulfonic ion exchange resins that had already been used for other applications, namely: Amberlyst 35dry, Amberlyst 36dry, Purolite CT275DR, Purolite CT276 and Lewatit GF101. Thorough characterization of the resins is herein provided and discussed, including acidity, elemental analysis, thermogravimetric, 13C-NMR, surface area and pore size distribution measurements. Lewatit GF101 showed the best performance reaching a yield to solketal of 47% after 6 h of operation at 313 K using a molar excess of acetone to glycerol of 4.5 to 1, owing to a greater availability of active centers as well as the ease of access to them than in the rest of the resins. Additionally, reutilization with and without regeneration was performed in up to five cycles, showing that Purolite CT276 had the lowest relative drop of its maximum activity, despite being the least active in each of the cycles.

Keywords: catalyst deactivation; glycerol; ion exchange resin; solketal; solventless synthesis.

1 Introduction

The philosophy of Green Chemistry is based on principles aimed at acting on the source to prevent pollution and misuse of resources. Thus, emphasis is put on waste prevention, use of safer solvents if any, employing catalysts and utilization of renewable feedstock [1]. Under a scenario in which glycerol is overabundant due to the current situation of the biodiesel market, new applications of this chemical have been searched for. Owing to its chemical structure and functionality, assorted chemicals have been obtained [2–4]. Among them are different glycerides [5, 6], 1,3-propanediol [7] or glycerol carbonate [8–11], which have all proven value-added products in different industries.

1,2-Isopropylideneglycerol, also referred to as solketal is one of such products. As a final product, it is put to use as a plasticizer, a green solvent and a suspending agent, especially in pharmaceutical preparations [12]. Moreover, its chemical reactivity makes it a feedstock to other chemicals of pharmaceutical interest like diglycerides, prostaglandins, glycerophospholipids or β-blockers like (S)-propranolol, extensively used for hypertension, migraine and other medical treatments [13, 14]. Undoubtedly, one of the most explored features of oxygenate derivatives from glycerol has been its use as a fuel additive [15–18]. In this context, solketal has been proven to enhance certain performance parameters and specifications. Reduced gum formation and improvement of the octane index were observed when using up to 5% volume of solketal to gasoline [19], while addition of said ketal to biodiesel not only improved its viscosity, but also complied with the flash point and oxidation stability specifications as enacted by European and American Standards (EN 14214 and ASTM D6751) [20]. Even further reactions of solketal have been explored to yield new potential additives, namely: its upgrade to benzyl alcohol ether [21] or the synthesis of solketal o-methylesters through the reaction with dialkyl carbonates under basic conditions [22].

While the synthesis of ketals has been pursued throughout the years, an increasing number of efforts have been made more recently. Ketalization consists of the reaction of an alcohol with ketones or aldehydes in an acidic medium; more specifically, cyclic ketals (like solketal) may be obtained through the reaction of polyols (like glycerol) with carbonyl moiety-containing compounds (like acetone), as depicted in Figure 1.

Considering the limited miscibility between glycerol and acetone in the initial stages of the reaction [23], many authors have followed an approach whereby the synthesis of solketal is conducted using cosolvents to limit mass

---

*Corresponding author: Jesús Esteban, School of Chemical Engineering, University of Birmingham, Edgbaston, Birmingham B15 2TT, UK, e-mail: J.EstebanSerrano@bham.ac.uk
Félix García-Ochoa and Miguel Ladero: Department of Chemical Engineering, College of Chemical Sciences, Complutense University of Madrid, 28040 Madrid, Spain
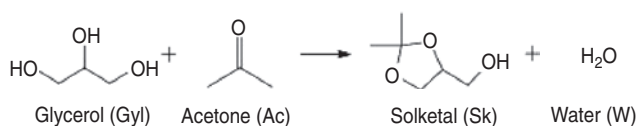
Figure 1: Acetalization of glycerol with acetone to yield solketal and water as a by-product.

transfer constrains between the two liquid phases that form and the solid phase of the heterogeneous catalyst [21, 24–27]. However, these mass transfer limitations can be overcome if the appropriate agitation rate and particle size of the catalyst are used [28].

A number of sulfonic-based ion exchange resins can provide the acidic medium necessary for the reaction subject of study to occur [29–34]. In this work, other resins that have proven of research interest have been tested. Purolite CT275 has been used for the synthesis of isopropyl tert-butylether from isopropanol and isobutene by means of an etherification reaction [29] or in membranes for the purification and drying of alcohols [30]. Purolite CT276 has been employed in water treatments for the removal of iodides together with Purolite CT275 [31]. The two mentioned Purolite resins along with Amberlyst 35 and Amberlyst 36 have been used in other reactions like the oligomerization of 1-hexene [32] and etherifications and dehydrations from alcohols [33]. Lewatit GF101 has only been reported thus far in the removal of free fatty acids in biodiesel manufacture processes and is, therefore, the one that lacks the most information [35].

Even more interestingly, the Amberlyst 35 and Amberlyst 36 resins have been found to be used in reactions involving the transformation of glycerol as a means to pursue its valorization. Amberlyst 35 has proven useful in etherification [36] and the production of triacetylglycerol by esterification and acetylation of glycerol [37] or even in the ketalization of glycerol to solketal in a solvent-based operation [32]. By contrast, the use of Amberlyst 36 has been reported for acetylation to yield products like monoacetates or polyacetates used in biodegradable polymers and products in the cosmetic and food industry [38].

The aim of this work is to continue the studies of glycerol valorization avoiding the use of solvents, following the premises of Green Chemistry. For this purpose, this work deals with the solventless synthesis of solketal through the reaction of glycerol with acetone using heterogeneous catalysts under mild conditions at temperatures below the boiling point of acetone. More importantly, an assessment of the performance and reutilization of commercially available ion exchange resins has been conducted together with some relevant characterization.

2 Materials and methods

2.1 Materials

2.1.1 Chemicals: Experiments were performed with extra pure glycerol (99%) (Scharlau Chemie Ltd, Barcelona, Spain) and acetone (HPLC grade) (Romil Ltd., Cambridge, UK). Preparation of samples required methanol (HPLC grade) (Fisher Scientific Ltd., Loughborough, UK) as internal standard and deuterium oxide (99.8%, NMR spectroscopy grade) (Scharlau Chemie Ltd., Barcelona, Spain) as solvent.

2.1.2 Catalysts: The following acidic ion exchange resins were employed: Purolite CT275DR, Purolite CT276 (Purolite Ltd., Cardiff, UK); Amberlyst 35dry, Amberlyst 36dry (Rom and Haas SAS, Lauterbourg, France) and Lewatit GF101 (Lanxess GmbH, Cologne, Germany), all of which were kindly supplied by each manufacturer. While all of the catalysts were supplied in their dry form, additional overnight drying at 373 K in a Heraeus Series 6000 (Thermo Fisher Scientific Ltd., Loughborough, UK) vacuum oven was conducted in order to ensure complete dryness prior to catalytic experiments.

2.2 Catalyst characterization

Brunauer-Emmett-Teller (BET) surface area of the resins was determined using the N2 adsorption-desorption technique at 196 K performed by a SA3100 analyzer (Beckman Coulter Ltd., High Wycombe, UK). Prior to the measurements, samples were degassed at 373 K during 120 min.

Porosimetry by mercury extrusion was completed for an approximate sample mass of 0.25 g of each resin in an Electron Pascal 440 series device (Thermo Scientific Ltd., Loughborough, UK) to quantify for mesopores and macropores. The calculation of the pore diameter was made using the Washburn cylindrical pore model, where the surface tension of mercury and the mercury contact angle were taken as 0.484 N/cm and 141°, respectively.

Thermogravimetric analyses were made in a 851e TGA/SDTA instrument (Mettler Toledo, Leicester, UK). Temperature was increased from 333 K to 833 K at a heating rate of 10 K/min under a nitrogen flow of 20 ml/min so as to keep an inert atmosphere. Each sample weighed approximately 10 mg. The curves obtained for the thermal decomposition of each catalyst were the average of three experiments.

Solid state ^{13}C-NMR spectroscopy of the catalysts was performed at 400 scans in a DSX300 MHz BACS60 device (Bruker Ltd., Coventry, UK) with an automatic sampler.

Elemental microanalysis was performed in a CHNS-932 equipment (LECO, Saint Joseph, MI, USA). Prior to the analysis of the resins, samples of 3 mg were dried overnight at 373 K to avoid errors due to the residual moisture.

For the potentiometric titration of the catalysts, a suspension of 25 mg of the resin in 40 ml of acetonitrile was prepared and kept under stirring for 24 h prior to the addition of a solution of N-butylamine in acetonitrile (0.005 N) at a constant flow rate of 0.4 ml/min. Potential was measured with an Eutech Instruments pH 700 pH-meter.

Additionally, Bronsted acidity of the resins was suspending overnight 10 mg of the resins in a solution of 7.5 g/l of KCl in water. The acid capacity was determined from measuring the pH value.

Table 1 compiles the physical and chemical properties of the resins determined from the aforementioned methods or as specified by the suppliers.

Table 1: Properties of the sulfonated ion exchange resins used for the synthesis of solketal.

Sample	Appearance	Maximum operating temperature (K)[a]	Acid capacity (eq H+ kg^{-1})[b]	BET surface area (m^2 g^{-1})[c]	Pore volume (cm^3 g^{-1})[d]	Surface area (m^2 g^{-1})[d]	Bulk density (g cm^{-3})[d]	Apparent density (g cm^{-3})[d]
GF101	Beige opaque solid	403	5.11	28	0.270	48	1.15	1.67
CT275DR	Brown opaque solid	453	4.98	29	0.434	45	1.00	1.77
CT276	Brown opaque solid	403	4.90	26	0.411	45	1.10	2.01
A35dry	Gray opaque solid	423	5.25	30	0.336	78	1.10	1.75
A36dry	Gray opaque solid	423	5.42	31	0.128	40	1.54	1.92

[a]From supplier.
[b]Obtained from ion exchange with NaCl.
[c]Obtained from BET; [d]from Hg porosimetry.

2.3 Apparatus and methodology

The experimental setup consisted of a glass reactor heated by means of a thermal resistor placed surrounding its outer walls with temperature being controlled by an OMRON E5CN PID controller linked to the resistor. Stirring of the system was regulated by a flat six-blade impeller on an IKA RW20 motor (250–2500 rpm) (IKA, Oxford, UK). Sample withdrawal was performed with a syringe with a wide-bore needle piercing a Teflon lid tightly fitted to the upper part of the reactor.

The operational procedure followed in all the experiments started by loading the reactants glycerol and acetone into the glass reactor. The catalyst was added when the set temperature was reached and samples were withdrawn thenceforth. The standard reaction conditions chosen for the study were a temperature of 313 K, a molar excess of acetone of 4.5 and a catalyst load of 0.5% of weight of catalyst per unit weight of the reactants (indicated as w/w onwards). In addition, the mode of operation of this reaction implies no removal of water as a reaction by-product to shift the equilibrium towards the products, considering the fact that it is known to be a major source of sulfonic acid-based ion exchange resins deactivation [39].

For the catalyst recycling experiments, up to four repetitions of the assay under the same conditions were completed. From experiment to experiment, the catalyst was filtered out of the reaction mixture, washed with methanol and dried at 373 K overnight. For catalyst regeneration, treatment with 10 ml of a solution containing hyperchloric acid (1 N) per gram of resin was completed.

2.4 Analysis of samples

Analysis of samples was performed by ^{1}H NMR spectroscopy with a BRUKER DPX 300MHz BACS60 (Bruker Ltd., Coventry, UK) device using methanol as an internal standard for quantification purposes and deuterium oxide as solvent for the samples.

Solketal was the chemical species monitored, the signal of which was quantified and related to the concentration present in the reaction sample using methanol as an internal standard. Figure 2 shows a representative spectrum of a reaction sample, with the peaks corresponding to the protons of every compound present in the sample properly identified.

3 Results and discussion

3.1 Characterization of ion exchange resins

Figure 3 plots the mercury intrusion curves (A) and its differentiated curve (B) performed for the determination of the pore size distribution. It can be observed that CT275DR and CT276 behave very similarly in the intrusion curve, with a maximum slope of the decrease of mercury volume intruded at a pore diameter between 65 nm and 80 nm, with a very narrow distribution and both can be said to be macroporous resins. A35dry and A36dry, by contrast,
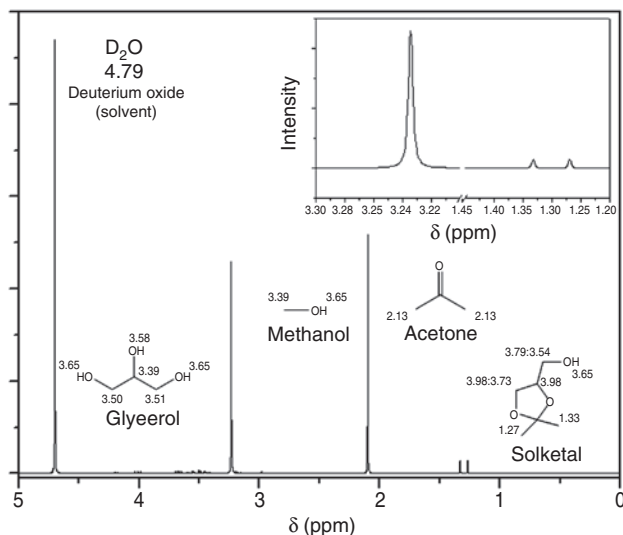
Figure 2: Representative ^{1}H-NMR spectrum 300 MHz spectra of a sample of the reaction with all the chemical components and shifts for the corresponding protons identified.
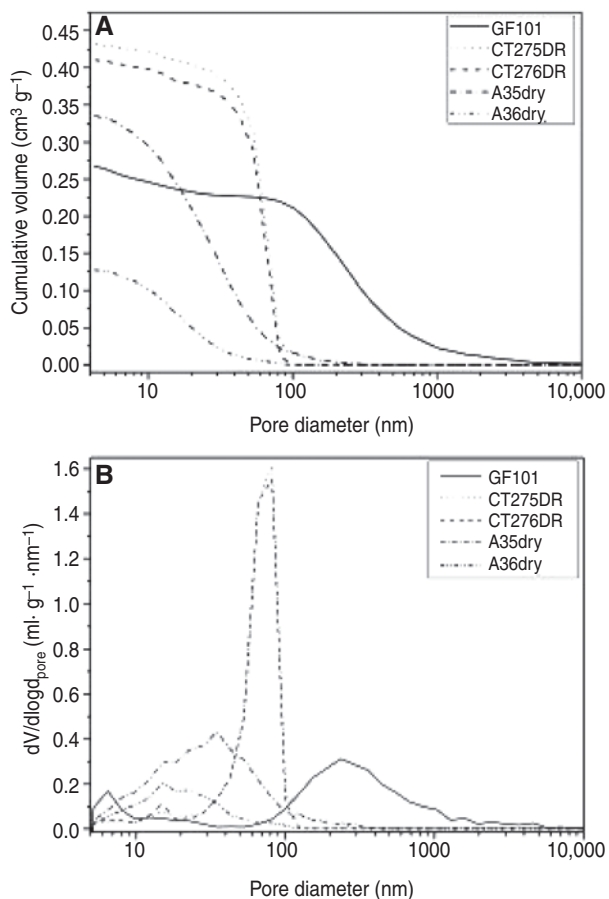
Figure 3: Mercury intrusion curves for the ion exchange resins (A) and pore size distribution derived from the intrusion curves (B).

show their drop at much lower pore diameters, reaching the maxima at approximately 35 nm and 15 nm, respectively, although with much wider pore size distributions than those observed for both Purolite resins. In the particular case of A35dry, there are an appreciable amount of pores above 50 nm, which means that this resin can be regarded as mesoporous and macroporous; on the contrary, the pore size distribution size of A36dry barely stretches beyond 43 nm, so it can be said that it is mainly a mesoporous resin. Finally, GF101 shows a somewhat different trend, with a bimodal pore size distribution with a relative maximum at 12 nm and an absolute maximum at 190 nm. Nevertheless, the preponderant fraction of pores ranges from slightly below 100 nm to 1000 nm; therefore, it can mostly be considered macroporous.

Thermograms of the ion exchange resins are plotted in Figure 4. Despite the similar behavior of the presented curves for all of the resins, the weight drop intervals vary from resin to resin. At temperatures up to 350 K, there is a typical slight weight loss due to the removal of moisture within the matrix of the samples. However, in this case, due to the dryness of these particular resins, these curves practically do not show this removal (not higher than 1–2% regardless of the resin considered). Neglecting this residual moisture removal interval, the curves exhibit a two-stage decay behavior with a middle step in which the weight remains almost constant. The first stage corresponds to a weight loss of 20–25%, ascribable to the degradation of sulfonic acids, the resin GF101 being the one with a lower quantity of sulfonic acids and similar groups containing sulfur. Maximum degradation rate in this temperature interval is attained at 355 K in all cases. The second stage weight drop can be attributed to the
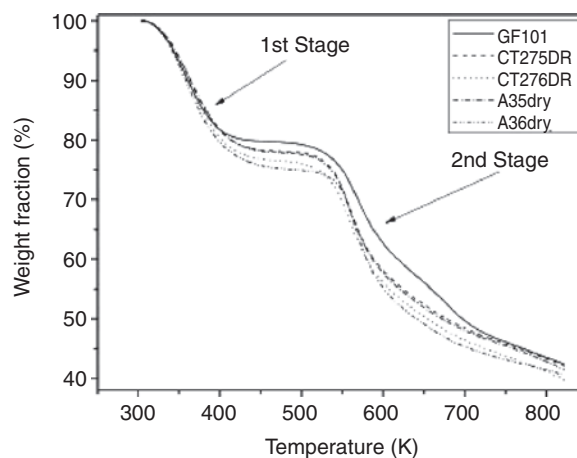
Figure 4: Thermal decomposition curves of the resins from 333 K to 823 K.

degradation of resin polymeric matrices, as described in several references [37, 38]. In resin GF101, as depicted in Figure 4, there are two weight loss zones within the 500–800 K temperature interval in GF101, indicating two different polymeric matrices in this resin, one of them slightly less stable than the other. In Figure 4, maximal degradation rates of the polymeric supports are observed at 555 K for Purolite resins, at 266 K for Amberlyst resins, and at 266 K and 677 K for the Lewatit GF101. Judging from these temperatures and the maximal degradation rates of the polymers, whose order is A36dry ≈ A35dry > CT276 > CT275 DR >> GF101, the thermal stability of the polymer in GF101 appears to be somewhat higher than the rest. At temperatures higher than 750 K, a low and constant degradation rate, similar for all resins, is observed.

Solid ^{13}C-NMR was performed to acquire a deeper knowledge on the presence of sulfonic groups within the structure of the resins. Figure 5 compiles the spectra obtained for the solid samples, where a series of representative signals can be seen. First, secondary and tertiary aliphatic carbons can be identified at a shift of
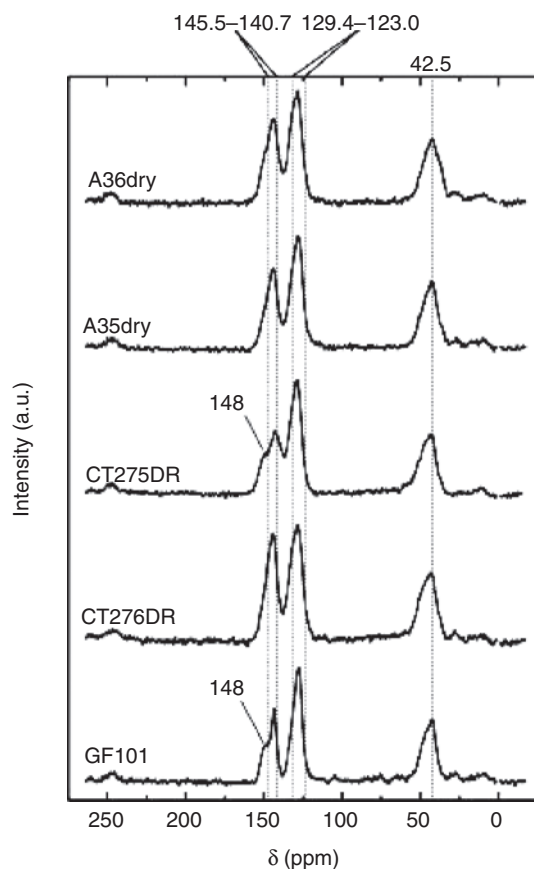
about 42.5 ppm, these being carbons accountable for the constitution of the backbone of the divinylbenzene structure [40]. Also, a signal, the maximum of which is at 127 ppm, is observed, which corresponds to the overlapping of the signals of aromatic carbon atoms at ortho- and meta-positions with respect to the carbon to which the sulfonic group is attached, which ranges between 123.0 ppm and 129.4 ppm as calculated in Table 2, considering the different carbons to which the sulfonic group can be attached [40, 41]. Finally, the peak at 140.7–145.5 ppm can be ascribed to directly alkylated or sulfonated carbon atoms, as estimated for the atoms a_1, b_1, a_2, c_2 and a_3 in Table 2; nevertheless, in the cases of CT275DR and GF101, a shoulder at 148 ppm appears. Detections at this value correspond to directly alkylated aromatic carbons at a para-position with respect to the sulfonated carbon atom, i.e. carbon atoms labeled as d_3 in Table 2. These signals at shifts very similar to the one reported herein corresponding to such type of carbon atoms in sulfonated solids have previously been reported [42, 43]. The greater the presence of these atoms, which appears to be more predominant in the mentioned resins, the more available the sulfonic group is owing to lower steric effects.

The elemental analysis of solids can also shed light on the presence of sulfonic groups. Figure 6 shows the elemental microanalysis performed for the resin samples, the oxygen weight fraction of which has been determined as the difference of the summation of the weight fraction of carbon, hydrogen, nitrogen and sulfur to 100%. The presence of sulfur ranges between 7% and 15%, CT275DR being the solid containing most sulfur, closely followed by GF101; A35dry and A36dry have similar sulfur content of 11.5% and 10.5%, respectively; finally, CT276 possesses the lowest content.

Finally, Figure 7 depicts the potentiometric titration of the five resins. According to Pizzio's classification, all of the resins have very strong sites given that the initial potential values are above 100 mV [44] and the order of strength would be as follows: CT275DR > A35dry > GF101 > A36dry > CT276. However, it is worthwhile mentioning the fact that the curves exhibit different behaviors. CT276, CT275DR and A35dry show a relatively slight reduction of the potential at the beginning of the titration and then a steep decrease; A36dry presents a similar curve, although the drop is not as pronounced as in the previous three cases. By contrast, GF101 shows a marked decline of the potential practically from the beginning. This can lead one to think that the acidity of the latter catalyst becomes available more quickly than the others and, thus, can be associated to the highest strength and catalytic activity.


Figure 5: ^{13}C-NMR spectra of the sulfonic resins with identifying guidelines (detailed in the text and Table 2).

Table 2: Estimated ^{13}C-NMR shifts for the carbon atoms of vinylbenzene sulfonated at *ortho-*, *meta-* and *para-* positions [40, 41].

Sulfonated vinylbenzene	Carbon atom	z_i^a (alkyl chain)	δ (ppm)	z_i^a (SO3H)	δ (ppm)	$δ_{total}$ (ppm)[a]
	a_1	z_2	− 0.6	z_1	15.0	142.9
	b_1	z_1	15.7	z_2	− 2.2	142.0
	c_1	z_2	− 0.6	z_3	1.3	129.2
	d_1	z_3	− 0.1	z_4	3.8	132.2
	e_1	z_4	− 2.8	z_3	1.3	127.0
	f_1	z_3	− 0.1	z_2	− 2.2	126.3
	a_2	z_3	− 0.1	z_1	15.0	143.4
	b_2	z_2	− 0.6	z_2	− 2.2	125.7
	c_2	z_1	15.7	z_3	1.3	145.5
	d_2	z_2	− 0.6	z_4	3.8	131.7
	e_2	z_3	1.3	z_3	− 0.1	129.7
	f_2	z_4	− 2.8	z_2	− 2.2	123.5
	a_3	z_4	− 2.8	z_1	15.0	140.7
	b_3	z_3	− 0.1	z_2	− 2.2	126.2
	c_3	z_2	− 0.6	z_3	1.3	129.4
	d_3	z_1	15.7	z_4	3.8	148
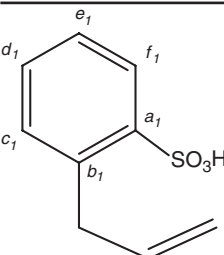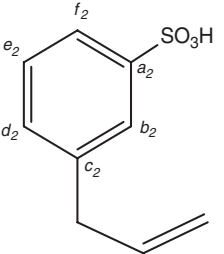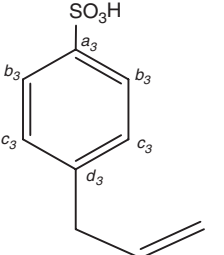
[a]Total shift was calculated according to $\delta_{total} = 128.5 + \sum_i z_i$, where 128.5 is the shift corresponding to any carbon atom in the benzene ring and z_i is the shift due to the presence of a substituent in the position i.
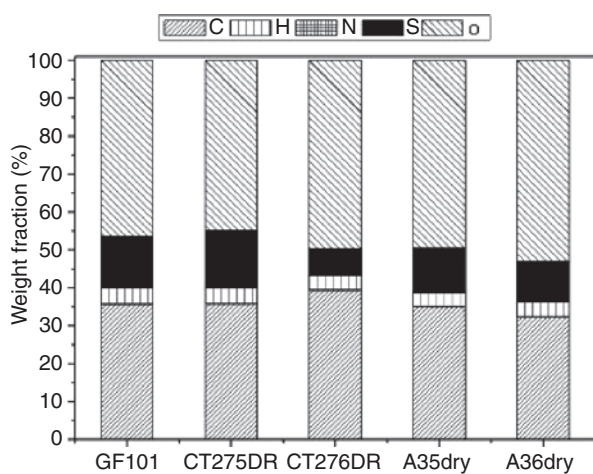
Figure 6: Elemental microanalysis of the ion exchange resins.
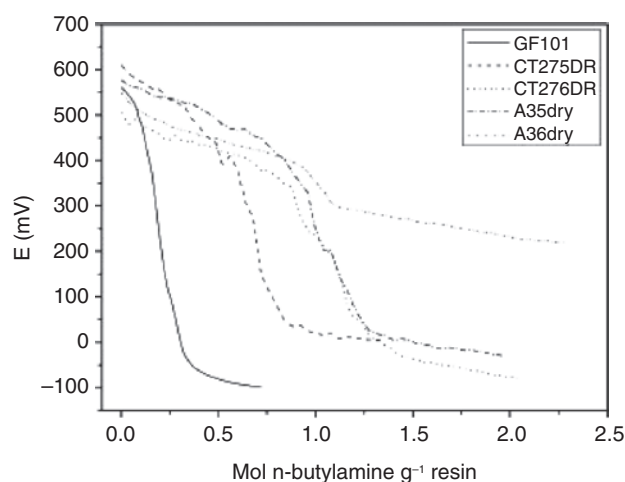
Figure 7: Potentiometric titration of the sulfonic acid-based ion exchange resins.

3.2 Catalytic experiments

The ionic exchange resins were tested for activity in the synthesis of solketal under solventless operation at a temperature of 313 K and a molar excess of acetone to glycerol of 4.5 to 1 with a catalyst load of 0.5% of weight of each resin per unit weight of the reactants. It is worthwhile

remarking on the fact that at this temperature and these composition conditions, the reacting system is immiscible to a high extent. Moreover, the reaction between acetone and glycerol does not take place in the absence of catalysts, as indicated in the liquid-liquid equilibria studies existing for the systems acetone + glycerol + solketal [23] and acetone + glycerol + water [45]. As the products of the reaction generate, solketal and water, the system turns into a single liquid phase. The reaction herein reported does not take place in the absence of catalysts, unless supercritical conditions are achieved [46].

Figure 8 shows the evolution of the yield to solketal obtained throughout assays with each of the resins, with yield being defined as the percentage of the ratio of the concentration of solketal at each moment to the initial concentration of glycerol. In addition to the five resins herein tested, Amberlyst 15 (A15) has been used as a reference. It is a well-known classic cation exchange resin existing for over 50 years which has been characterized [47] and used in the dehydration-hydrogenation of xylose [48] or the acetylation of glycerol, a relatively similar reaction [38]. From the plot, it can be seen that the reaction reaches its equilibrium position at approximately 5 h only when GF101 is used; however, after 6 h, equilibrium is still not reached in the cases of CT275DR, A35dry, A36dry and A15, which exhibited similar performance, and CT276.

The inset graph of Figure 8 shows the progress of the reaction within the first hour of the reaction. The shapes of the curves are typical of those obtained using heterogeneous catalysts. It can be seen that, from the very beginning of the reaction, the performance observed for GF101 is better than the rest. This observation could be explained
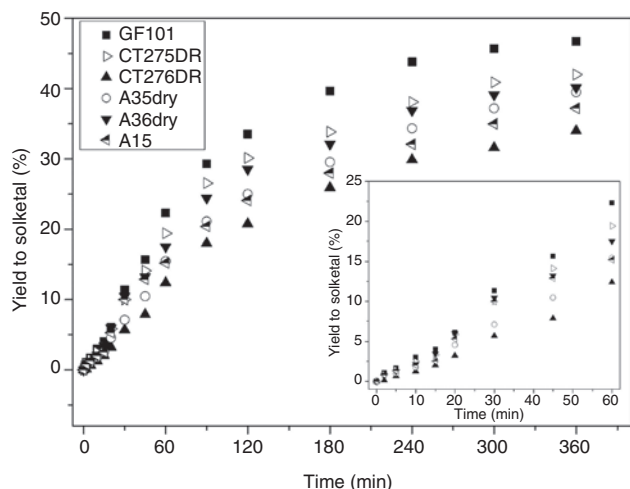
given the features described for this throughout Section 3.1. As shown by mercury porosimetry, this resin exhibits a bimodal pore distribution size curve, with an absolute maximum at 190 μm, yet with a distribution around this size that spreads well across the macroporous region. At short times of reaction, there is still a liquid-liquid biphasic system due to the limited miscibility between the two reactant species; therefore, the viscosity of glycerol plays an important role. GF101 possesses a much wider macroporous region, which in turn facilitates the access of glycerol into the pores. In addition, the solid ^{13}C-NMR analysis showed that the presence of sulfonic groups in para-positions with respect to the vinyl matrix is significant in GF101 as well as in CT275DR, the resin with the second best performance. These results also agree with the results obtained from the elemental microanalysis, in which the presence of sulfur was the highest for these two resins and the lowest for CT276, the least active catalyst. Moreover, the potentiometric titration and the acid capacity of the resins also show that GF101 has a greater acidity. In summation, the availability of the active acid sites appears to be the key aspect to explain the performance of these catalysts, despite the fact that the two most active resins do not possess the highest pore volume or surface area within their structures (see Table 1).

Additionally, the effect that the presence of water generated as a byproduct may exert on the catalyst has to be taken into account. Resins based on sulfonic acids like Amberlyst 15, Amberlyst 16 and Dowex Wx8 have been tested for deactivation in the presence of water [49–53], reaching the conclusion that there is a high affinity of sulfonic acids for water. This could explain the deactivation of the catalyst with time as well as the fact that the equilibrium conversion is difficult to shift towards the products and only reaches approximately 47%.

The performance of this reaction using these catalysts appears to be lower than in other studies present in the literature. Nevertheless, some of these studies report on the production of solketal following strategies that remove water (by-product of the reaction) from the medium as a means to shift the reaction towards the products. For instance, conversions of glycerol as high as 81% have been attained using ZrO2-SiO2 as a catalyst operating under reactive distillation at 343 K [54]; 84% employing Ar-SBA15 also at 343 K in three consecutive two-step batches under reflux and subsequent evaporation of water under vacuum [55]; 82% using montmorillonite K10 withdrawing water with a zeolite-based membrane [56] or 90% with p-toluenesulfonic acid applying a reactive distillation strategy [20]. In other cases, the strategy followed was to include solvents as part of the reaction medium, which

Figure 8: Yield to solketal obtained for each of the tested catalysts at 313 K, a molar excess of acetone to glycerol of 4.5 and a catalyst load of 0.5% w/w.

affects the activity coefficients of each component in the medium, leading to different equilibrium conversions. In this way, Nanda et al. [32] achieved a 65% conversion using Amberlyst 35 at 323 K using methanol as solvent and Menezes et al. [57] a 66% conversion with $SnCl_2$ at 333 K in the presence of acetonitrile under reflux operation. In the case of the present study, it must be acknowledged that these conditions under a mode of operation with no water removal and absence of solvents had not been tried previously to test the endurance of the catalysts.

3.3 Reutilization of the catalyst

A series of recycling assays was performed in order to assess the stability of the resins to deactivation throughout consecutive experiments. The activity of the resins was considered as the turnover frequency (TOF) observed for each resin at each cycle, established as:

$$TOF = \frac{r_{max}}{C_{cat}} \qquad (1)$$

where r_{max} is the maximum reaction rate observed (mol·l^{-1}·min^{-1}) and C_{cat} the equivalent concentration of protons (mol·l^{-1}), obtained from the acid capacity of the resins (Table 1).

After observing the evolution of the yield to solketal in the inset of Figure 8, the evolution of the concentration of solketal with respect to time was fitted making use of the Hoerl curve [58] to the kinetic data obtained in successive recycling experiments, as defined by Eq. (2):

$$C_{Sk} = A \cdot B^t \cdot t^C \qquad (2)$$

where C_{Sk} is the concentration of solketal (mol·l^{-1}), t is time and A, B and C are the fitting parameters of the equation. From the differentiation of Eq. (2), the reaction rate as a function of time is obtained, the maximum value of which is herein considered as r$_{max}$ to be used in Eq. (1).

Table 3 shows the evolution of the TOF of each resin vs. the number of recycling experiments. It can be observed that GF101 has the highest activity in practically all the cycles followed by CT275DR, as already addressed. Nonetheless, it is worthwhile mentioning that as the reutilization of the catalysts progresses, the activity of these two resins approaches similar values to those obtained by the rest of the catalysts.

Figure 9 emphasizes on these findings. This graph plots the remaining activities referred to as the first use of each resin as a function of the total operating time. Each cycle was performed for 2 h in these reutilization experiments. It can be seen that a regeneration of the catalyst with perchloric acid improves to some extent the remaining activity with respect to the non-regenerated catalyst. The remaining activities of the non-regenerated and regenerated resins have been fitted relatively well to an exponential decay model of the following type:

$$a_r = A \cdot exp(-k_d \cdot t) \qquad (3)$$

in which a_r is the remaining activity, t refers to the total operating time of the resin and A and k_d are the amplitude and the decay constant, i.e. the fitting parameters of the curve.

Table 4 compiles the values of the mentioned parameters as well as the half-life period. This value corresponds to the number of cycles at which the model predicts that the remaining activity will be equal to 0.5.

Both in Figure 9 and from the half-life value in Table 4 it can be inferred that GF101 suffers the highest decrease in activity despite showing the best performance in all the cycles. CT275DR, A35dry, A36dry and A15 have all similar half-life values of around six cycles. Curiously, the least active species in this work, i.e. CT276, showed the lowest decay in activity with only a loss of 18% after the first four cycles when no regeneration was made and 24% when such a procedure was performed, reaching lower, although somewhat similar values to those obtained for silica-included heteropolyacids, where the activity drop

Table 3: Evolution of turnover frequency (TOF) of the resins with recycling experiments at 313 K, M = 4.5 and catalyst load of 0.5% w/w.

Cycle						TOF (min⁻¹)
	Lewatit GF101	**Purolite CT275DR**	**Purolite CT276DR**	**Amberlyst 35dry**	**Amberlyst 36dry**	**Amberlyst 15**
1	0.41313	0.38241	0.2351	0.30476	0.26605	0.2541
2	0.36908	0.33534	0.21633	0.26476	0.21587	0.2342
3	0.2865	0.30924	0.20204	0.24267	0.20517	0.2111
4	0.28063	0.26827	0.19469	0.20076	0.18155	0.1822
5	0.20861	0.20643	0.15959	0.17067	0.15461	0.1646

TOF = turnover frequency.
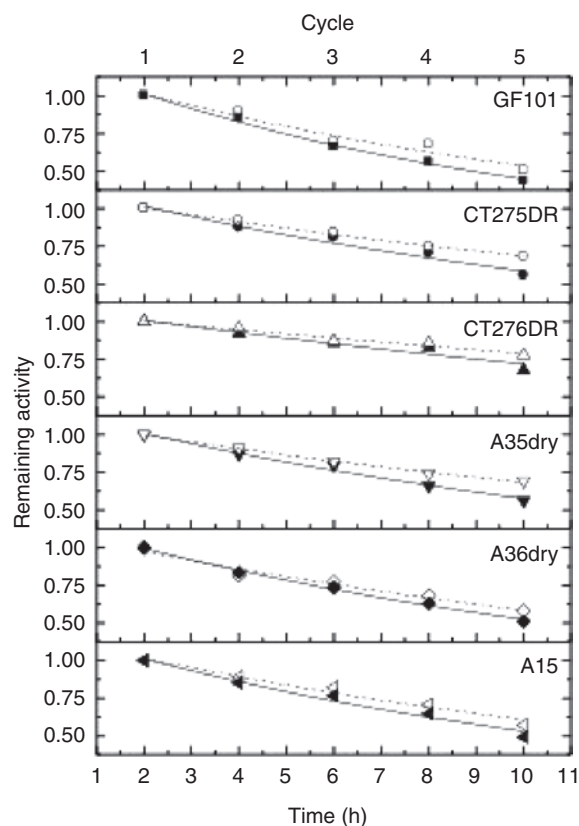
Figure 9: Progress of the experimental and fitted remaining activity with total operating time and number of recycles of the catalysts. Solid markers correspond to regenerated catalysts, open markers correspond to non-regenerated.

identical in what regards stability if technical-grade glycerol is employed, expecting a rapid deactivation of the catalyst if crude glycerol is the reagent. The latter result can be explained by cation exchange between sodium and protons, as crude glycerol is rich in sodium salts [55].

4 Conclusions

A series of commercially available sulfonic ion exchange resins were employed to convert glycerol and acetone to solketal in the absence of solvents. The five resins herein tested showed accepted performance in completing the reaction. Thorough characterization of the resins was conducted, revealing that Lewatit GF101, followed by Purolite CT275DR, had the highest sulfur content and provided the best accessibility and availability of sulfonic active sites despite not showing the highest surface area among the resins tested. The order of activity of the resins observed could be explained by such mentioned features of the resins. The order of activity is as follows, including the traditional resin Amberlyst 15: Lewatit GF101 > Purolite CT275DR > Amberlyst 35dry > Amberlyst 36dry > Amberlyst 15 > Purolite CT276.

Reutilization of the catalysts was also performed through an assessment of the decrease of the TOF after successive recycles with and without regeneration of the catalyst. In this case, evaluation of the half-life of the remaining activity of the reused and regenerated catalysts revealed that the order of stability was very different to the performance, namely: Purolite CT276 > Amberlyst 36dry > Amberlyst 15 > Purolite CT275DR > Amberlyst 35dry > Lewatit GF101.

was estimated to be up to 13% after the same number of reutilization cycles [59].

For the present study, high purity glycerol was used to ensure maximum activities and stabilities for the catalysts tested. However, results are expected to be almost

Table 4: Summary of the parameters used for the remaining activity exponential decay model [Eq. (3)] and half-life period for the regenerated and non-regenerated catalyst.

Regeneration of catalyst	Catalyst	A ± error	k_d ± error	r^2	$t_{1/2}$ (h)
No	GF101	1.19 ± 0.07	0.08 ± 0.01	0.94	10.82
	CT275DR	1.16 ± 0.05	0.07 ± 0.01	0.95	12.32
	CT276	1.10 ± 0.04	0.04 ± 0.01	0.91	18.58
	A35dry	1.16 ± 0.03	0.07 ± 0.02	0.98	12.03
	A36dry	1.11 ± 0.04	0.07 ± 0.01	0.96	12.49
	A15	1.15 ± 0.05	0.07 ± 0.02	0.96	12.36
Yes	GF101	1.24 ± 0.03	0.10 ± 0.01	0.99	8.93
	CT275DR	1.19 ± 0.04	0.08 ± 0.02	0.98	10.28
	CT276	1.13 ± 0.03	0.06 ± 0.01	0.97	14.37
	A35dry	1.20 ± 0.03	0.08 ± 0.01	0.99	10.51
	A36dry	1.17 ± 0.02	0.08 ± 0.01	0.99	10.62
	A15	1.19 ± 0.04	0.08 ± 0.02	0.98	10.55

References

[1] Anastas P, Warner J. *Green Chemistry Theory and Practice*, Oxford University Press: New York, 2008.

[2] Zhou C-H, Beltramini JN, Fan Y-X, Lu GQ. *Chem. Soc. Rev.* 2008, 37, 527–549.

[3] Behr A, Eilting J, Irawadi K, Leschinski J, Lindner F. *Green Chem.* 2008, 10, 13–30.

[4] Pagliaro M, Rossi M. *The Future of Glycerol: New Uses of a Versatile Raw Material*, RSC Publishing: Cambridge, UK, 2008.

[5] Molinero L, Ladero M, Tamayo JJ, Esteban J, Garcia-Ochoa F. *Chem. Eng. J.* 2013, 225, 710–719.

[6] Tamayo JJ, Ladero M, Santos VE, Garcia-Ochoa F. *Process Biochem.* 2012, 47, 243–250.

[7] Li Y, Liu H, Ma L, He D. *RSC Adv.* 2014, 4, 5503–5512.

[8] Esteban J, Ladero M, González-Miquel M, Fuente E, Blanco A, García-Ochoa F. *RSC Adv.* 2014, 4, 53206–53215.

[9] Esteban J, Dominguez E, Ladero M, Garcia-Ochoa F. *Fuel Process. Technol.* 2015, 138, 243–251.

[10] Esteban J, Fuente E, Blanco A, Ladero M, Garcia-Ochoa F. *Chem. Eng. J.* 2015, 260, 434–443.

[11] Esteban J, Ladero M, Fuente E, Blanco Á, García-Ochoa F. *J. Taiwan Inst. Chem. Eng.* 2016, 63, 89–100.

[12] Budavari S, In *Merck Index*, 11th ed., Merck & Co. Inc.: Rahway, New Jersey, 1989.

[13] Jurczak J, Pikul S, Bauer T. *Tetrahedron* 1986, 42, 447–488.

[14] Hof RP, Kellogg RM. *J. Org. Chem.* 1996, 61, 3423–3427.

[15] Karinen RS, Krause AOI. *Appl. Catal. A- Gen.* 2006, 306, 128-133.

[16] Klepáčová K, Mravec D, Kaszonyi A, Bajus M. *Appl. Catal. A-Gen.* 2007, 328, 1–13.

[17] Melero JA, van Grieken R, Morales G, Paniagua M. *Energ. Fuels* 2007, 21, 1782–1791.

[18] Rahmat N, Abdullah AZ, Mohamed AR. *Renew. Susta. Energ. Rev.* 2010, 14, 987–1000.

[19] Mota CJA, da Silva CXA, Rosenbach N, Jr., Costa J, da Silva F. *Energ. Fuels* 2010, 24, 2733–2736.

[20] Garcia E, Laca M, Perez E, Garrido A, Peinado J. *Energ. Fuels* 2008, 22, 4274–4280.

[21] Suriyaprapadilok N, Kitiyanan B. *Energ. Proc.* 2011, 9, 63–69.

[22] Selva M, Benedet V, Fabris M. *Green Chem.* 2012, 14, 188–200.

[23] Esteban J, Vorholt AJ, Behr A, Ladero M, Garcia-Ochoa F. *J. Chem. Eng. Data* 2014, 59, 2850–2855.

[24] Nanda MR, Yuan Z, Qin W, Ghaziaskar HS, Poirier M-A, Xu C. *Fuel* 2014, 128, 113–119.

[25] Nanda MR, Yuan Z, Qin W, Ghaziaskar HS, Poirier M-A, Xu C. *Appl. Energ.* 2014, 123, 75–81.

[26] Nanda MR, Yuan Z, Qin W, Ghaziaskar HS, Poirier M-A, Xu CC. *Fuel* 2014, 117, 470–477.

[27] Shirani M, Ghaziaskar HS, Xu C. *Fuel Process. Technol.* 2014, 124, 206–211.

[28] Esteban J, Ladero M, García-Ochoa F. *Chem. Eng. J.* 2015, 269, 194–202.

[29] Tejero J, Creus E, Iborra M, Cunill F, Izquierdo JF, Fite C. *Catal. Today* 2001, 65, 381–389.

[30] Korzh RV, Bortyshevskii VA, Tkachenko TV, Evdokimenko VA, Boiko VV. *Russ. J. Appl. Chem.* 2007, 80, 1335–1340.

[31] Tsao HW, In *Method of Iodide Removal*, The Purolite Company: Cardiff, UK, 2009.

[32] Cadenas M, Bringue R, Fite C, Ramirez E, Cunill F. *Top. Catal.* 2011, 54, 998–1008.

[33] Bringue R, Ramirez E, Iborra M, Tejero J, Cunill F. *J. Catal.* 2013, 304, 7–21.

[34] da Silva CXA, Mota CJA. *Biomass Bioenerg.* 2011, 35, 3547–3551.

[35] Ramírez-López C, Nieto-Maestre J, Gómez-Jiménez-Aberasturi O, Ochoa-Gómez JR, Arteche-Calvo A, Belsue M, Aragón JJ, Dobarganes MC, Ruiz-Méndez MV, Production of biodiesel from high acidic raw materials. Design and development of an heterogeneous catalytic process, in: ANQUE International Congress of Chemical Engineering Seville (Spain), 2012.

[36] Turan A, Hrivnak M, Klepatova K, Kaszonyi A, Mravec D. *Appl. Catal. A-Gen.* 2013, 468, 313–321.

[37] Liao X, Zhu Y, Wang S-G, Li Y. *Fuel Process. Technol.* 2009, 90, 988–993.

[38] Dosuna-Rodriguez I, Gaigneaux EM. *Catal. Today* 2012, 195, 14–21.

[39] Kale S, Umbarkar SB, Dongare MK, Eckelt R, Armbruster U, Martin A. *Appl. Catal. A-Gen.* 2015, 490, 10–16.

[40] Dean J. *Analytical Chemistry Handbook*, McGraw-Hill: New York, 1995.

[41] Ewing DF. *J. Org. Magn. Reson.* 1979, 12, 499–524.

[42] Sadaba I, Ojeda M, Mariscal R, Lopez Granados M. *Appl. Catal. B-Env.* 2014, 150, 421–431.

[43] Lopez Granados M, Carolina Alba-Rubio A, Sadaba I, Mariscal R, Mateos-Aparicio I, Heras A. *Green Chem.* 2011, 13, 3203–3212.

[44] Pizzio LR, Vazquez PG, Caceres CV, Blanco MN. *Appl. Catal. A-Gen.* 2003, 256, 125–139.

[45] Krishna R, Low CY, Newsham DMT, Oliverafuentes CG, Paybarah A. *Fluid Phase Equilib.* 1989, 45, 115–120.

[46] Royon D, Locatelli S, Gonzo EE. *J. Supercrit. Fluids* 2011, 58, 88–92.

[47] Kunin R, Fisher SA, Meitzner EF, Frisch N, Oline JA. *Ind. Eng. Chem. Prod. RD* 1962, 1, 140–144.

[48] Ordomsky VV, Khodakov AY, Nijhuis AT, Schouten JC. *Green Process. Synth.* 2015, 4, 369-377.

[49] Tesser R, Casale L, Verde D, Di Serio M, Santacesaria E. *Chem. Eng. J.* 2010, 157, 539–550.

[50] Park JY, Kim DK, Lee JS. *Bioresour. Technol.* 2010, 101, S62–S65.

[51] Park JY, Wang ZM, Kim DK, Lee JS. *Renew. Energ.* 2010, 35, 614–618.

[52] Popken T, Gotze L, Gmehling J. *Ind. Eng. Chem. Res.* 2000, 39, 2601–2611.

[53] Ali SH, Tarakmah A, Merchant SQ, Al-Sahhaf T. *Chem. Eng. Sci.* 2007, 62, 3197–3217.

[54] Fan C, Xu C, Liu C, Huang Z, Liu J, Ye Z. *Heterocycles* 2012, 85, 2977–2986.

[55] Vicente G, Melero JA, Morales G, Paniagua M, Martin E. *Green Chem.* 2010, 12, 899–907.

[56] Roldan L, Mallada R, Fraile JM, Mayoral JA, Menendez M. *Asia-Pacific J. Chem. Eng.* 2009, 4, 279–284.

[57] Menezes FDL, Guimaraes MDO, da Silva MJ. *Ind. Eng. Chem. Res.* 2013, 52, 16709–16713.

[58] Hoerl AE. Fitting curves to data. In *Chemical Business Handbook*; Perry JH, Ed., McGraw-Hill: New York, 1954; pp 55–57.

[59] Ferreira P, Fonseca IM, Ramos AM, Vital J, Castanheiro JE. *Appl. Catal. B-Env.* 2010, 98, 94–99.

Bionotes

Jesús Esteban

Jesús Esteban studied Chemical Engineering at the Complutense University of Madrid (Spain), where he earned his PhD degree in 2015. As part of his thesis, he authored nine articles dealing with physicochemical aspects of processes devoted to the chemical valorization of glycerol to value-added products, thanks to which he received the award for the best PhD thesis in Science and Technology of the Royal Academy of Doctors of Spain in 2015 and the Green Talents Award sponsored by the German Federal Ministry of Education and Research in 2016. In addition, he received a grant from the German Academic Exchange Service (DAAD) to undertake a research stay at the Technical University of Dortmund. As of 2016, he is a postdoctoral research fellow at the University of Birmingham, where he studies the interaction between powders and liquid surfactants in addition to continuing work on the characterization and application of glycerol-derived products.

Félix García-Ochoa

Félix García-Ochoa obtained his PhD in Industrial Chemistry in 1977 and is at present a full professor of Chemical Engineering at the Complutense University of Madrid (Spain). Throughout his career in research, he has been the author of over 150 papers (h index = 32) and as many conference communications. Among other institutions, he has received grants from the German Academic Exchange Service (DAAD), the British Council and the Fulbright Foundation in addition to having been awarded the Gold Medal of the National Chemists Association of Spain (ANQUE) and the Gold Medal of the Spanish Royal Society of Chemistry (RSEQ). In 2017, he will act as Chairman of the Scientific Committee of the 10th World Congress of Chemical Engineering (WCCE10).

Miguel Ladero

Miguel Ladero received his PhD in Industrial Chemistry in 1999. Presently, he is an associate professor of Chemical Engineering at the Complutense University of Madrid. His main research interests focus on process optimization and intensification, catalytic and biocatalytic processes, biorefinery processes, mass transfer and biocatalyst immobilization, resulting, as of 2016, in the supervision of five PhD theses and over 50 MSc and BSc theses. He has over 30 contributions in Q1-Q2 JCR journals, and over 100 contributions to international congresses, patents and conferences. He has participated in a total of 16 national and international (Era-net) projects and four contracts with private organizations, performing the project leader role in four of them.